Nonthermal Irreversible Electroporation as a Focal Ablation Treatment for Brain Cancer

15

Paulo A. Garcia, John H. Rossmeisl Jr., Thomas L. Ellis, and Rafael V. Davalos

Contents

Abstract

Irreversible Electroporation (IRE) is a new focal tissue ablation technique that has shown great promise as a treatment for a variety of soft-tissue neoplasms. The therapy uses pulsed electric fields to destabilize cell membranes and achieve tissue death in a non-thermal manner. The procedure is minimally invasive and is performed through small electrodes inserted into the tissue with treatment duration of about 1 min. In this chapter we describe the first systematic in vivo studies of IRE in canine brain tissue. We confirmed that the procedure can be applied safely in the brain and was well tolerated clinically in normal dogs. The necrotic lesions created with IRE were sub-millimeter in resolution, sharply delineated from normal brain, and spared the major blood vessels. In addition, our preliminary results in a rodent study indicate that IRE transiently disrupts the BBB adjacent to the

P.A. Garcia (✉)
School of Biomedical Engineering and Sciences,
Virginia Tech – Wake Forest University,
330 ICTAS Building, Stanger Street,
Blacksburg, VA 24061, USA
e-mail: pgarcia@vt.edu

J.H. Rossmeisl Jr.
Department of Small Animal Clinical Sciences,
Virginia-Maryland Regional College of Veterinary Medicine, 205 Duck Pond Drive,
Blacksburg, VA 24061, USA

T.L. Ellis
Department of Neurosurgery, Wake Forest University School of Medicine, 1 Medical Center Blvd,
Winston-Salem, NC 27157, USA

R.V. Davalos
School of Biomedical Engineering and Sciences,
Virginia Tech – Wake Forest Universitye,
329 ICTAS Building, Stanger Street,
Blacksburg, VA 24061, USA

M.A. Hayat (ed.), *Tumors of the Central Nervous System, Volume 12*,
DOI 10.1007/978-94-007-7217-5_15,

ablated area in a voltage-dependent manner with implications for enhanced delivery of cytotoxic agents to regions with infiltrative tumor cells. Finally, we present representative case examples demonstrating therapeutic planning aspects, clinical applications, and results of IRE ablation of spontaneous malignant intracranial gliomas in canine patients. Our group has demonstrated that IRE ablation can be performed safely, and is effective at reducing the tumor volume and associated intracranial hypertension, and allows for improvement in tumor-associated neurologic dysfunction. Our work illustrates the potential benefits of IRE for in vivo ablation of neoplastic brain tissue, especially when traditional methods of cytoreductive surgery are not possible or ideal.

Introduction

High-grade gliomas, most notably glioblastoma multiforme (GBM), are among the most aggressive of all malignancies in humans and dogs. High-grade variants of gliomas are difficult to treat and generally considered incurable with singular or multimodal therapies (Stupp et al. 2005; La Rocca and Mehdorn 2009). Many patients with GBM die within 1 year of diagnosis, and the 5-year survival rate in people is approximately 10 % (Stupp et al. 2005). Despite extensive research and advancement in diagnostic and therapeutic technologies, very few therapeutic developments have emerged that have significantly improved survival for humans with GBM over the last seven decades (Stupp et al. 2005).

Considering the therapeutic challenge that neurosurgeons are faced with when managing patients with malignant glioma (MG), many recent efforts have been directed into the development of minimally invasive techniques that can be used for focal neoplastic tissue ablation as alternatives to traditional surgical approaches. Thermal-dependent tissue ablation techniques, such as cryoablation (Tacke 2001), laser interstitial thermotherapy (Atsumi et al. 2001), and radiofrequency lesioning (Cosman et al. 1983) have been developed, but with limited success or applicability in the brain primarily due to the heat sink effect associated with the vascular brain parenchyma.

Irreversible electroporation (IRE) is a new technique for the focal ablation of undesirable tissue with pulsed electric fields (Al-Sakere et al. 2007). One of the main advantages of IRE over other focal ablation techniques is that the therapy does not rely on temperature changes to kill the cells (Garcia et al. 2011b), a process which is also referred to as non-thermal irreversible electroporation (N-TIRE). The thermal sparing effect of IRE is advantageous compared to previously described methods of tissue destruction that are dependent on local tissue temperature changes and results in sparing of major blood vessels, extracellular matrix, and other critical structures within the treated tissue (Al-Sakere et al. 2007).

An IRE treatment involves placing minimally invasive electrodes within the region of interest and delivering a series of electric pulses that are microseconds in duration (Lee et al. 2007). The pulses create an electric field that induces an increase in the resting transmembrane potential (TMP) of the cells in the tissue (Davalos et al. 2005). The induced increase in the TMP is dependent on the electric pulse (e.g. strength, duration, repetition rate, shape, and number), impedance distribution of the tissue as well as the tissue type, and physical configuration of the electrodes used to deliver the pulses. Depending on the magnitude of the induced TMP, as well as its duration and repetition rate for induction, the electric pulses can have no effect, transiently increase membrane permeability, or cause cell death. Spatially, for a given set of conditions, the TMP and therefore the degree of electroporation is dependent on the local electric field and the tissue type to which the cells are exposed. Because the transitions in cellular response to the electric pulses are sudden, the treated regions are sharply delineated. Consequently, numerical models that simulate the electric field distributions in tissue can be used to predict the treated region (Miklavcic et al. 2000; Edd and Davalos 2007).

Recently, IRE has shown promise as a therapy for soft-tissue neoplasms, using minimally invasive instrumentation and allowing for treatment

monitoring with routine clinical procedures (Ball et al. 2010; Neal et al. 2011; Thomson et al. 2011). Studies of focal IRE ablations in mammalian liver and prostate have shown that therapeutic protocols are safe and can be implemented to preserve the integrity of sensitive tissues, such as the major vasculature and ductal frameworks within treated parenchymal volumes (Lee et al. 2007; Onik et al. 2007; Rubinsky et al. 2007; Appelbaum et al. 2012; Ben-David et al. 2012). We believe that the IRE technology possesses other inherent properties that make it well suited for the treatment of brain lesions in which the therapeutic intent is focal and highly controlled tissue destruction.

This chapter presents results on the first in vivo experimental use of IRE to ablate normal brain (Ellis et al. 2011) demonstrating the safety, vascular sparing, and other focal ablative characteristics of intracranial IRE procedures. We also present preliminary data on the duration and extent of blood–brain-barrier (BBB) disruption surrounding an IRE-induced zone of ablation in rodents (Garcia et al. 2012). Finally, we describe applications of IRE for the in vivo treatment of inoperable spontaneous canine intracranial MGs, highlighting its potential for more widespread clinical usage for the ablation of neoplastic brain tissue (Garcia et al. 2011a). Our studies have demonstrated the ability of IRE to safely ablate pathologically heterogeneous brain tissue while preserving vascular integrity and patient neurological functions. We illustrate the minimally invasive nature of IRE and the ability to plan and execute IRE therapy using procedures routinely used in clinical evaluation of neurosurgical patients.

Safety Study

Treatment Parameters

The safety study was approved by the Virginia Tech Institutional Animal Care and Use Committee (IACUC). The dogs were systemically healthy and neurologically intact prior to the study, based on normal physical and neurologic examinations, results of complete blood counts, and serum biochemistry profiles. No abnormalities were detected on scalp-recorded electroencephalograms (EEG) and baseline magnetic resonance imaging (MRI) examinations of the brain. After administration of general anesthesia, neuromuscular blockade, and an anti-convulsant (phenobarbital 6 mg/kg IV), routine craniectomies were performed to expose the right parietotemporal region of the brain of each dog. Focal ablative IRE lesions were created in the ectosylvian gyrus using a NanoKnife™ pulse generator and blunt tip electrodes (AngioDynamics®, Queensbury, NY USA).

For dog 1, a single probe (1.65 mm diameter) with both an energized and ground contact was used at a depth of 2 mm below the gyral surface. For the remaining test dogs smaller dual probes (1.0 mm diameter) were used at a depth of 7 mm below the cortex, where one probe was energized and the other grounded. IRE lesions were created by administering nine sets of ten 50-μs pulses at a rate of 4 pulses per second. The pulses were configured with alternating polarity between each set to minimize total charge delivered to the brain. The strength of the electric field is dependent on the applied voltage and electrode configuration which are given in Table 15.1. The voltage and

Table 15.1 Pulse parameters used in safety study of intracranial IRE in normal canine brain (Adapted from Ellis et al. (2011))

Dog	Blunt tip electrodes	Electrode exposure [mm]	Separation distance [mm]	Voltage [V]	Total pulses
1	Single	7 and 5.3	8	1,600	9×10
2	Dual	5	5	1,000	9×10
3	Dual	5	5	500	9×10
4 – Control	Dual	5	5	1,000	9×10
	Dual	5	10	2,000	9×10
5 – Control	Dual	5	5	0	0

pulse parameters were determined from the literature and from ex vivo experiments on canine brain (Al-Sakere et al. 2007; Lee et al. 2007; Onik et al. 2007). The animals were treated with 1,600, 1,000, and 500 V, respectively in order to assess whether lower voltages could still produce ablations.

One control animal (Dog 4) was treated at a higher voltage to evaluate the upper safety limit of the procedure by delivering ~4.5× more energy than in Dog 2 (Ellis et al. 2011). In this animal, two lesions were created using the dual electrode configuration at applied voltages of 1,000 and 2,000 V. The last animal was used as a sham control to examine the physical effects of electrode insertion without pulse delivery. Non-energized electrodes were advanced into the brain and maintained in place for approximately 30 s, the time required to deliver the IRE pulses in the other animals.

Neurologic, Imaging, and Histopathological Evaluation

After the IRE procedure, the animals were evaluated and treated in the standard fashion for post-craniectomy canine patients. There was no significant deterioration in neurologic ability or coma scale scores from baseline evaluations. The animals were able to ambulate and eat within 10 h of the procedure. No seizures were observed. Analysis of the intra-operative ultrasound obtained for each animal revealed a clearly demarcated hypoechoic zone with hyperechoic rim within the targeted brain parenchyma which was consistent with results in other organs (Lee et al. 2007; Appelbaum et al. 2012; Schmidt et al. 2012).

MRI examinations performed immediately post-operatively revealed fluid accumulation within the ablation sites and a focal disruption of the BBB (Fig. 15.1). These images also show that the IRE ablation zones were sharply demarcated and iso- to hypointense on T1-weighted sequences, hyperintense on T2-weigthed sequences, and markedly and contrast enhancing following intravenous administration of gadolinium.

The IRE lesion in the brain of Dog 1 was more superficial than the lesions in the other animals, due to the depth of insertion of the electrodes. In this animal, a single probe was inserted parallel to the surface of the brain at a depth of 2 mm. Grossly visible brain edema and surface blanching of the gyrus overlying the inserted electrode were observed within 2 min of completion of the IRE procedure. This edema resolved completely following intravenous administration of 1.0 g/kg of 20 % mannitol. Because of these effects, the subsequent animals were treated with a smaller dual probe configuration with electrodes inserted perpendicular to the brain surface at a 7-mm depth. Brain edema and surface blanching were not observed during treatment of the remaining dogs.

The microscopic lesions from the histopathology correlated well with the gross appearance and MRI sequences in dogs 1–3. A histological comparison between the sham control and dog 3 revealed that the isolated effect of electrode insertion was limited when compared to the IRE lesion. Histopathologic sections also demonstrated that the IRE lesions have a sub-millimeter line of demarcation between areas of necrosis and normal brain. The areas of treatment were represented by foci of malacia and dissociation of white and grey matter. Small perivascular hemorrhages were present although there was sparing of major blood vessels. High-voltage pulses in dog 4 were associated with non-selective coagulative necrosis of all tissues within the treatment field, resulting in lacunar infarction secondary to arterial thrombosis. Moderate diffuse perivascular and intraglial edema, reactive gliosis, as well as death of neuronal and glial cells were also observed. The treatment area was moderately infiltrated with mixed inflammatory cells, including neutrophils, macrophages, plasma cells, and small lymphocytes. Smaller lesions were observed when decreasing the voltage between dogs. As a result, customizing the pulse parameters should allow the ablation of volumes with varying sizes and shapes.

The ablations were confirmed with histopathological analysis, revealing a sub-millimeter boundary between the necrotic and normal brain. Reconstructed lesion volumes of 1.655, 0.599, and 0.258 cm^3 were calculated from the post-operative T2W MRIs using open source image

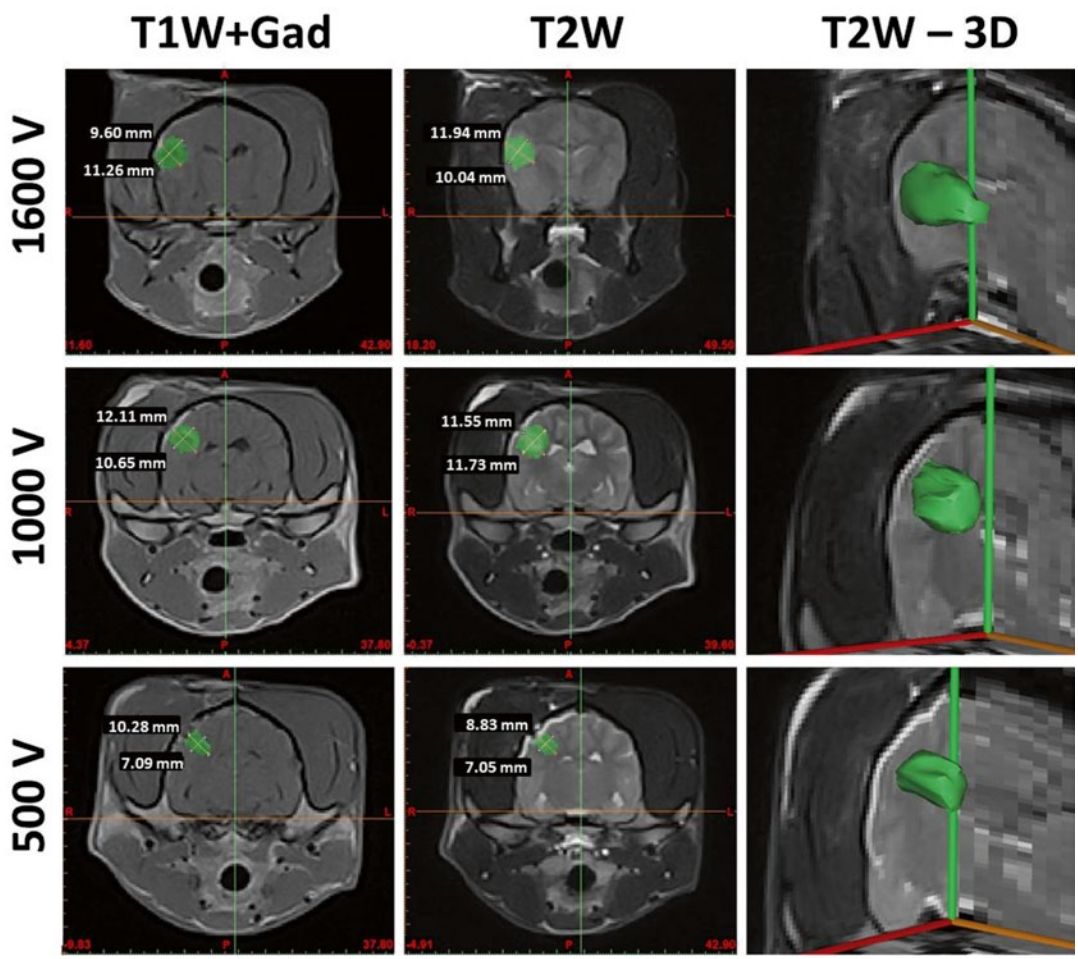

Fig. 15.1 MRI characteristics of focal brain ablations induced by IRE. Lesions (*green shading*) are well demarcated from surrounding brain parenchyma, homogenously T2 hyperintense, and markedly enhanced on TIW post-contrast images. There is a positive correlation between lesion size and the applied voltages

analysis software (OsiriX, Geneva, Switzerland). The accuracy of the computed lesion volumes was limited to the interval between the MRI scans (2.5–3.0 mm). It is important to note that the volumes of the lesions were reconstructed from MRIs taken within 60 min after pulse administration, so the observed ablation volume is likely to be that resulting from immediate IRE induced cellular necrosis (Garcia et al. 2011b). This means that any additional cellular death resulting from late-onset apoptosis may not be taken into account in the electric field correlation (Garcia et al. 2011b). Our results support the hypothesis that IRE can be used safely in the brain and that lesion volume can be correlated with applied voltage. In this canine study, as in other studies of soft-tissue organs, IRE associated edema developed following treatment. Although the vasogenic edema observed on the MRI of dogs in this study was not associated with any clinical deterioration, it is a cause of concern. Brain edema after IRE should be anticipated and treated with perioperative corticosteroids.

IRE may offer advantages over surgical resection for selected brain tumors. The small electrode size makes the procedure minimally invasive and adaptable to virtually any neuroanatomic location

with existing stereotactic guidance systems. IRE creates a sharply delineated volume of ablated tissue with sub-millimeter resolution that may make it suitable for treating deep-seated, well-circumscribed brain tumors. The minimal heat generation during treatment and sparing of major blood vessels may also make it appropriate for tumors adjacent to, or enveloping critical vascular structures. The following two sections in the chapter describe representative treatment planning procedures and clinical applications of IRE for the treatment of canine patients with spontaneous brain cancer.

Treatment Planning

Some of the advantages of IRE over other focal ablation techniques are that the treated regions are highly predictable and the technique does not depend on thermal changes to achieve tissue death (Al-Sakere et al. 2007; Ahmed et al. 2011). The extent of IRE is determined by the impedance distribution of the tissue as well as the tissue type, electrode-tissue geometry, and pulse parameters including strength, duration, number, shape, and repetition rate. However, for a given set of pulse conditions, the primary parameters affecting the degree of electroporation are the tissue type and the local electric field distribution (Edd and Davalos 2007). Therefore, the electric field distribution must be determined in order to design effective protocols for IRE procedures. Furthermore, to verify that specific protocols do not induce thermal damage due to excessive Joule heating, the temperature distribution can also be calculated from the electric field distribution and the thermal properties of the tissue. Knowledge of the electric field and temperature distribution enables researchers and physicians to reliably predict the results of an IRE procedure and minimize damage to surrounding healthy tissue. This insight enables surgeons to plan and optimize the electrode configuration and pulse parameters to:

1. Perform IRE treatment planning using medical images
2. Minimize applied voltages in order to reduce charge delivered
3. Avoid inducing thermal damage due to excessive Joule heating
4. Reduce treatment time, invasiveness, and number of procedures
5. Ensure coverage of the entire tumor, especially when multiple applications are needed

In this section we outline the IRE treatment planning procedures for canine patients with brain cancer. Specifically we describe the tissue segmentation, volumetric meshing, and finite element modeling used for therapeutic planning prior to surgical procedures.

Segmentation and Meshing of Tissue Components

Mimics 14.1 image analysis software (Materialise, Leuven, BG) is used to segment the brain tumor geometry from normal brain tissue components including the ventricles and the white and gray matter. The tumor is traced in each of the two-dimensional (2-D) diagnostic MRI, CT, or any other DICOM format imaging modalities according to intensity values. A three-dimensional (3-D) solid representation of the tumor volume, the ventricles, and the brain tissue is then refined and exported to 3-matic version 6.1 (Materialise, Leuven, BG) in order to generate a volumetric mesh for the computational models. The refined volumetric meshes are then imported into a finite element modeling (Comsol Multiphysics, v.4.2a, Stockholm, Sweden) software in order to simulate the physical effects of the electric pulses in the tumor and surrounding normal brain tissue.

Finite Element Modeling of Electric Field Distribution

The methods used to generate the electric field distributions in tissue are similar to the ones described by Edd and Davalos (2007). The electric field distribution associated with the electric pulse is given by solving the Laplace equation:

$$\nabla \cdot (\sigma \nabla \varphi) = 0 \tag{15.1}$$

where σ is the electrical conductivity of the tissue and φ is the electrical potential (Edd and Davalos 2007). Boundary conditions most often include surfaces where electric potential is specified, as in the case of a source or sink electrode, or surfaces that are electrically insulating, as on the free surfaces of the tissue, for example. The electrical boundary condition along the tissue that is in contact with the energized electrode is $\varphi = V_o$. The electrical boundary condition at the interface of the other electrode is set to ground. The remaining boundaries are treated as electrically insulating:

$$\frac{\partial \varphi}{\partial n} = 0 \tag{15.2}$$

The models are fully defined and readily solvable using numerical methods once an appropriate set of boundary conditions, initial conditions, and physical properties of the tissue are defined. The computations are performed with a commercial finite element package (Comsol Multiphysics 4.2a, Stockholm, Sweden). The analyzed domain extends far enough from the area of interest (i.e. the area near the electrodes) that the electrically insulating boundaries at the edges of the domain do not significantly influence the results in the treatment zone.

The numerical models have been adapted to account for a dynamic non-linear tissue conductivity that occurs as a result of electroporation and redistributes the electric field during the treatment (Garcia et al. 2010, 2011a, b; Neal et al. 2012). The significant non-linear changes in the electrical conductivity of treated tissues occur because of cell membrane defects that facilitate the flow of ions and current through cells and are necessary in order to accurately represent IRE treatments. The dynamic conductivity, $\sigma(E,T)$, is a function of the electric field (E) and temperature (T) of the tissue during the IRE treatment. In tissue and tumors, this increase in conductivity is approximately 3×–6× the baseline conductivity when fully electroporated (Ivorra et al. 2009; Neal et al. 2012) and needs to be determined for normal and pathologic brain tissue components.

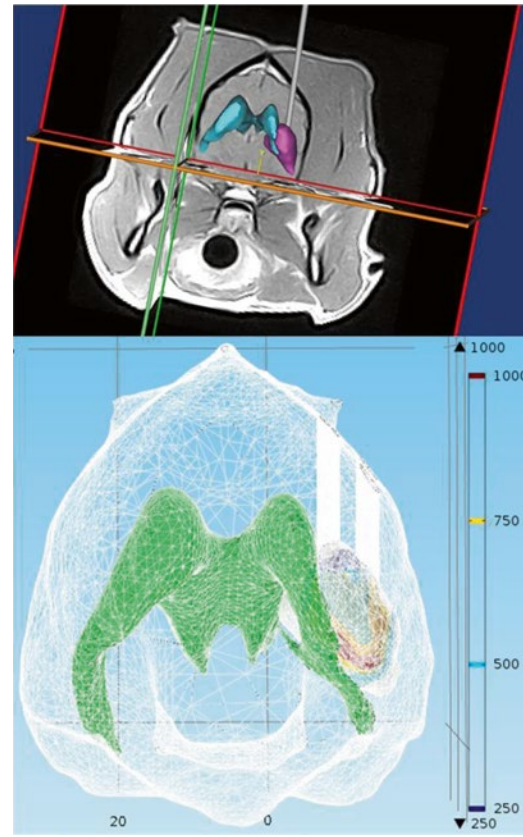

Fig. 15.2 Imaging-based computational models for treatment planning and optimization of IRE procedures in canine patients with brain cancer with (*top*) 3D reconstructed tissue components and the (*bottom*) simulated electric field distribution [V/cm]

Based on the tumor dimensions and computational simulations, IRE pulse parameters are determined to ensure coverage of the entire tumors and minimize damage to the surrounding healthy tissue. The resulting electric field distributions from these parameters can be visualized in Fig. 15.2. We are currently evaluating the electric field threshold in a clinical IRE study of canine patients with MG and are using the method proposed by Neal et al. (2012) to determine the non-linear conductivity function used in the finite element simulations. The promising clinical results that we have achieved in these patients suggest that our simulations are correct and that the electric field threshold used is capable of killing the tumor tissue.

Therapeutic Application

Dogs with spontaneous brain tumors have been shown to be excellent translational models of human disease. Canine malignant gliomas exhibit similar clinical, biologic, pathologic, molecular, and genetic properties as their human counterparts (Stoica et al. 2004; Dickinson et al. 2006; Rossmeisl et al. 2007). Here we illustrate the therapeutic application of IRE for treatment of MG using canines with spontaneous supratentorial gliomas. These canine patients are typically referred to our academic veterinary neurosurgical service for evaluation of tumor associated-seizures and interictal motor, sensory, and/or behavioral dysfunction referable to a focal intracranial neuroanatomic lesion following documentation of solitary intra-axial mass lesions with MR imaging characteristics consistent with gliomas (Fig. 15.3a-top panels); (Garcia et al. 2011a; Young et al. 2011). Prior to IRE therapy, peritumoral edema is treated with diuretics and corticosteroids, and anticonvulsants are administered as indicated.

Irreversible Electroporation Therapy

We use two general techniques to deliver IRE to canine MG, with the technique selection based on patient specific factors such as the volume and neuroanatomic location of the tumor, and the type and severity of any tumor-related complications (peritumoral edema, intratumoral hemorrhage, brain herniation, etc.). The first technique uses routine craniectomy approaches, similar to that described in our safety study (Fig. 15.3a-middle panels). The second is a minimally invasive, stereotactic approach in which a customized polymeric array is fabricated to accommodate the optimal electrode trajectory and configuration to a patient's specific tumor. The polymeric array is then implanted into the skull and the electrodes passed through the array into the tumor target during treatment (Fig. 15.3b-top panels). The polymeric array also provides a readily accessible and minimally invasive means for objective pathological evaluation of the tumor response through serial biopsy (Fig. 15.3b-bottom panels).

Total intravenous general anesthesia is induced and maintained with propofol and fentanyl constant rate infusions. Following biopsy of the tumor, neuromuscular blocking agents are administered to effect. The tumor is then ablated according to patient-specific treatment planning protocols (Table 15.2) using the NanoKnife™ (AngioDynamics®, Queensbury, NY USA), and blunt tip electrodes (1.0 mm diameter). Pulse delivery is synchronized with the electrocardiogram (ECG) signal to prevent ventricular fibrillation or other cardiac arrhythmias (Ivy Cardiac Trigger Monitor 3000, Branford, CT, USA). Pulse sets are delivered with alternating polarity between the sets to reduce charge build-up on the surface of individual electrodes. In addition, shorter pulse durations than those used in IRE studies (Al-Sakere et al. 2007; Onik et al. 2007; Rubinsky et al. 2007) outside the central nervous system (CNS) are used in order to reduce the charge delivered to the tissue and decrease resistive heating during the procedure. Our calculations and temperature measurements from previous intracranial IRE procedures ensure that no thermal damage is induced (Garcia et al. 2011b).

Post-IRE Evaluations

Objective tumor responses are evaluated using serial clinical neurologic examinations, brain MRI, and neuropathological studies. As illustrated in the acute post-treatment MR images (Fig. 15.3a-middle panels and Fig. 15.3b-bottom left panel), IRE therapy results in rapid reduction in contrast-enhancing tumor volumes and intracranial pressure without causing or exacerbating intratumoral hemorrhage or peritumoral edema. Neuropathological examinations of IRE treated MG (Fig. 15.3b-right panels) reveal near uniform neoplastic cell death and obliteration of tumor architecture. The scarce neoplastic cells with identifiable individual features within IRE ablated regions demonstrate apoptotic features

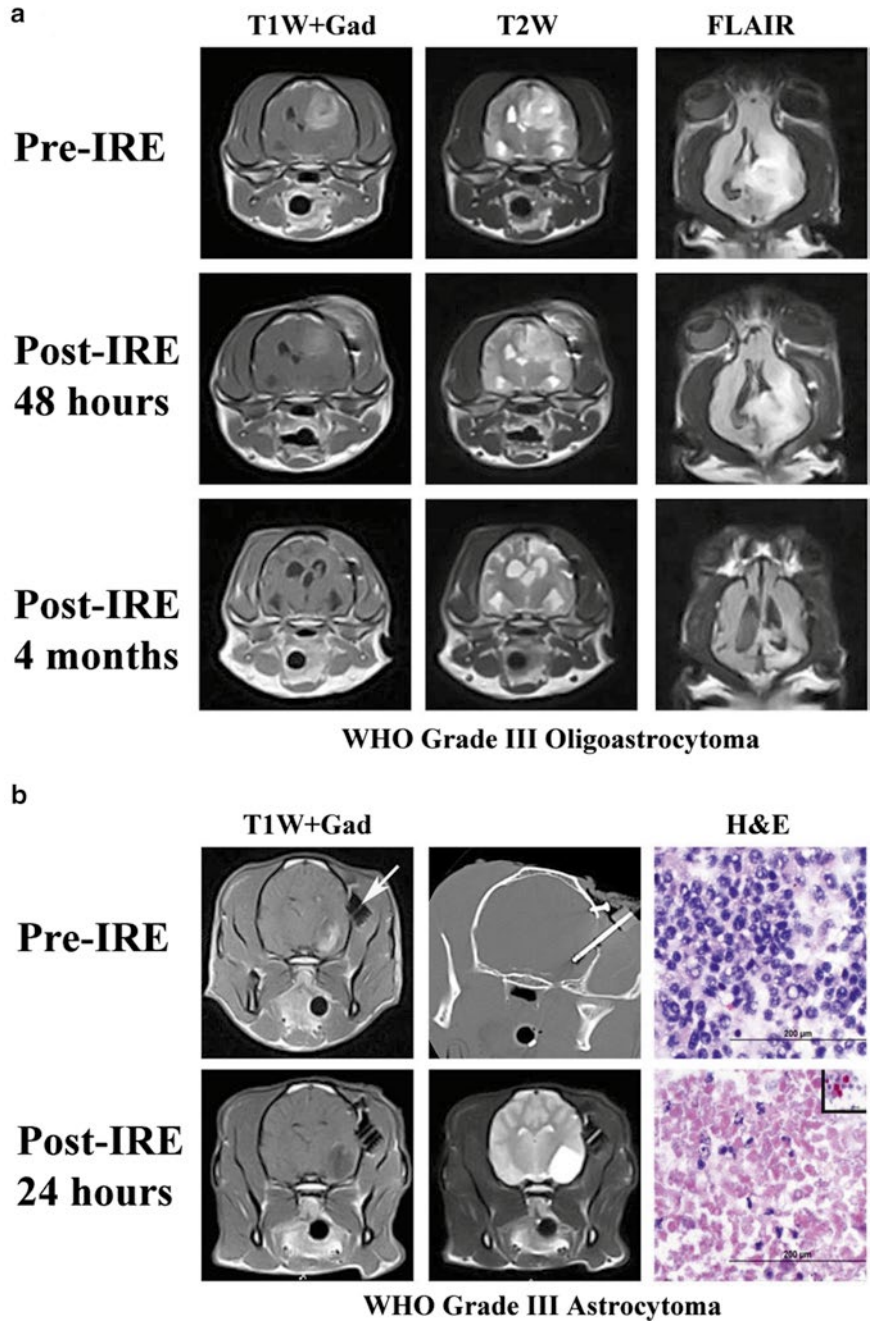

Fig. 15.3 MRI (**a**) and histologic (**b**) characteristics of focal tumor ablation before and after IRE treatment in canine patients with spontaneous malignant gliomas

(Fig. 15.3b, bottom right panel), and caspase-3 immunoreactivity (Fig. 15.3b, bottom right panel inset). These objective tumor responses are associated with acute post-operative improvements in neurological functions and overall clinical performance scores. The initial canine patient with MG treated with IRE and adjunctive radiation therapy at our institution experienced complete remission

Table 15.2 Representative IRE treatment protocol for canine patients with malignant glioma patient (Adapted from Garcia et al. (2011a))

Voltage (V)	Electrode gap (cm)	Electrode exposure (cm)	Volt-to-dist ratio (V/cm)	Pulse duration (μs)	Number of pulses	Frequency
500	0.5	0.5	1,000	50	2×20	ECG synchronized
625	0.5	0.5	1,250	50	4×20	ECG synchronized

(Fig. 15.3a-bottom panels), but did ultimately succumb to complications associated with radiation encephalopathy (Garcia et al. 2011a).

Discussion

Despite advances in cancer treatment, MG remains highly resistant to therapy. By nature of their neuroinvasiveness, MG are often not amenable to curative surgery and recur with high frequency (Stoica et al. 2004; Stupp et al. 2005; La Rocca and Mehdorn 2009). Even with aggressive multimodal treatment most patients succumb to the disease within 1 year. The 5-year survival rate for human patients with GBM is 10 % and this statistic has remained nearly unchanged over the last 70 years (Stupp et al. 2005). Although much less is known regarding the effects of single or multimodal therapies on the survival of dogs with gliomas, the prognosis is considered poor for dogs with MG, with one study reporting a median survival of 9 days for all dogs with non-meningeal origin neoplasms (Heidner et al. 1991).

IRE is a new minimally invasive technique to focally ablate undesired tissue using low energy electric pulses (Al-Sakere et al. 2007). These pulses permanently destabilize the membranes of the tumor cells, achieving death without inducing thermal damage in a precise and controllable manner with sub-millimeter resolution (Al-Sakere et al. 2007; Garcia et al. 2011a). The application of IRE requires minimal time and can be performed at the time of surgery or using stereotactic image (i.e. CT or MRI) guidance (Garcia et al. 2011b). This is an ideal treatment strategy for brain cancer patients where either tumor volumes are often sufficiently large to preclude safe traditional surgical excision without associated significant perioperative morbidity; or excision is not possible due to the neuroanatomic location of the tumor. We believe that, in addition to the ability to effectively ablate tissue in a non-thermal manner, a major advantage of IRE treatment is the very sharp transition between treated and non-treated tissue, which allows for sparing of sensitive neuroanatomic structures in proximity to the treatment field.

This chapter described the first systematic in vivo study of IRE for intracranial surgery (Ellis et al. 2011). We also presented the therapeutic planning aspect and implementation of IRE for treating canine patients with spontaneous brain tumors (Garcia et al. 2011a). Our results support the hypothesis that IRE can be used safely in the brain and that lesion volume can be correlated with applied voltage (Garcia et al. 2010; Ellis et al. 2011). IRE is a non-thermal ablation technique that kills tissue in a focal manner depicted by MR imaging and transiently disrupts the BBB adjacent to the ablated area in a voltage-dependent manner. In a rodent study in the brain we have also determined the extent and duration of the BBB disruption (Garcia et al. 2012) which will be critical for enhanced delivery of cytotoxic agents to regions with infiltrative tumor cells, especially high grade gliomas.

In conclusion, we have successfully shown that IRE is safe for use within the sensitive intracranial environment. The advantages of IRE over other focal ablation techniques lay within its ability to ablate tissue through a non-thermal mechanism. This method preserves the extracellular matrix, major blood vessels, and other sensitive tissues, enhancing treatment outcome. The IRE treatment is rapid, minimally invasive, and can be monitored using ultrasound, CT, and MRI. In addition, the lesions are sharply delineated between treated and non-treated tissue and are

sub-millimeter in resolution. Using a canine spontaneous model of MG, our group has developed and continues to refine IRE treatment planning and delivery methods that are effective for focal ablation of normal and neoplastic brain tissue.

Acknowledgments The work highlighted in this chapter was supported by the Coulter Foundation, the Golfer's Against Cancer, and by the CBET-0933335 and CAREER CBET-1055913 awards from the National Science Foundation (NSF) in the United States of America. The authors would also like to thank AngioDynamics® Inc. for loan of their equipment and for technical support of these studies.

References

Ahmed M, Brace CL, Lee FT Jr, Goldberg SN (2011) Principles of and advances in percutaneous ablation. Radiology 258(2):351–369

Al-Sakere B, Andre F, Bernat C, Connault E, Opolon P, Davalos RV, Rubinsky B, Mir LM (2007) Tumor ablation with irreversible electroporation. PLoS One 2(11):e1135

Appelbaum L, Ben-David E, Sosna J, Nissenbaum Y, Goldberg SN (2012) Us findings after irreversible electroporation ablation: radiologic-pathologic correlation. Radiology 262(1):117–125

Atsumi H, Matsumae M, Kaneda M, Muro I, Mamata Y, Komiya T, Tsugu A, Tsugane R (2001) Novel laser system and laser irradiation method reduced the risk of carbonization during laser interstitial thermotherapy: assessed by MR temperature measurement. Lasers Surg Med 29(2):108–117

Ball C, Thomson KR, Kavnoudias H (2010) Irreversible electroporation: a new challenge in "out of operating theater" anesthesia. Anesth Analg 110(5):1305–1309

Ben-David E, Appelbaum L, Sosna J, Nissenbaum I, Goldberg SN (2012) Characterization of irreversible electroporation ablation in in vivo porcine liver. Am J Roentgenol 198(1):W62–W68

Cosman ER, Nashold BS, Bedenbaugh P (1983) Stereotactic radiofrequency lesion making. Appl Neurophysiol 46(1–4):160–166

Davalos RV, Mir LM, Rubinsky B (2005) Tissue ablation with irreversible electroporation. Ann Biomed Eng 33(2):223–231

Dickinson PJ, Roberts BN, Higgins RJ, Leutenegger CM, Bollen AW, Kass PH, LeCouteur RA (2006) Expression of receptor tyrosine kinases vegfr-1 (flt-1), vegfr-2 (kdr), egfr-1, pdgfra and c-met in canine primary brain tumours. Vet Comp Oncol 4(3):132–140

Edd JF, Davalos RV (2007) Mathematical modeling of irreversible electroporation for treatment planning. Technol Cancer Res Treat 6:275–286

Ellis TL, Garcia PA, Rossmeisl JH Jr, Henao-Guerrero N, Robertson J, Davalos RV (2011) Nonthermal irreversible electroporation for intracranial surgical applications. Laboratory investigation. J Neurosurg 114(3):681–688

Garcia PA, Pancotto T, Rossmeisl JH, Henao-Guerrero N, Gustafson NR, Daniel GB, Robertson JL, Ellis TL, Davalos RV (2011a) Non-thermal irreversible electroporation (N-TIRE) and adjuvant fractionated radiotherapeutic multimodal therapy for intracranial malignant glioma in a canine patient. Technol Cancer Res Treat 10(1):73–83

Garcia PA, Rossmeisl JH Jr, Neal RE 2nd, Ellis TL, Davalos RV (2011b) A parametric study delineating irreversible electroporation from thermal damage based on a minimally invasive intracranial procedure. Biomed Eng Online 10(1):34

Garcia PA, Rossmeisl JH, Neal RE II, Ellis TL, Olson J, Henao-Guerrero N, Robertson J, Davalos RV (2010) Intracranial nonthermal irreversible electroporation: in vivo analysis. J Membr Biol 236(1):127–136

Garcia PA, Rossmeisl JH Jr, Robertson JL, Olson JD, Johnson AJ, Ellis TL, Davalos RV (2012) 7.0-T Magnetic resonance imaging characterization of acute blood–brain-barrier disruption achieved with intracranial irreversible electroporation. PLoS ONE 7(11):e50482

Heidner GL, Kornegay JN, Page RL, Dodge RK, Thrall DE (1991) Analysis of survival in a retrospective study of 86 dogs with brain tumors. J Vet Intern Med 5(4):219–226

Ivorra A, Al-Sakere B, Rubinsky B, Mir LM (2009) In vivo electrical conductivity measurements during and after tumor electroporation: conductivity changes reflect the treatment outcome. Phys Med Biol 54(19):5949–5963

La Rocca RV, Mehdorn HM (2009) Localized BCNU chemotherapy and the multimodal management of malignant glioma. Curr Med Res Opin 25(1):149–160

Lee EW, Loh CT, Kee ST (2007) Imaging guided percutaneous irreversible electroporation: ultrasound and immunohistological correlation. Technol Cancer Res Treat 6(4):287–294

Miklavcic D, Semrov D, Mekid H, Mir LM (2000) A validated model of in vivo electric field distribution in tissues for electrochemotherapy and for DNA electrotransfer for gene therapy. Biochim Biophys Acta 1523(1):73–83

Neal R II, Garcia P, Robertson J, Davalos R (2012) Experimental characterization and numerical modeling of tissue electrical conductivity during pulsed electric fields for irreversible electroporation treatment planning. IEEE Trans Biomed Eng 99:1

Neal RE II, Rossmeisl J, Garcia PA, Lanz O, Henao-Guerrero N, Davalos RV (2011) A case report on the successful treatment of a large soft-tissue sarcoma with irreversible electroporation. J Clin Oncol 29:1–6

Onik G, Mikus P, Rubinsky B (2007) Irreversible electroporation: implications for prostate ablation. Technol Cancer Res Treat 6(4):295–300

Rossmeisl JH, Duncan RB, Huckle WR, Troy GC (2007) Expression of vascular endothelial growth factor in tumors and plasma from dogs with primary intracranial neoplasms. Am J Vet Res 68(11):1239–1245

Rubinsky B, Onik G, Mikus P (2007) Irreversible electroporation: a new ablation modality–clinical implications. Technol Cancer Res Treat 6(1):37–48

Schmidt CR, Shires P, Mootoo M (2012) Real-time ultrasound imaging of irreversible electroporation in a porcine liver model adequately characterizes the zone of cellular necrosis. HPB 14(2):98–102

Stoica G, Kim HT, Hall DG, Coates JR (2004) Morphology, immunohistochemistry, and genetic alterations in dog astrocytomas. Vet Pathol 41(1):10–19

Stupp R, Mason WP, van den Bent MJ, Weller M, Fisher B, Taphoorn MJ, Belanger K, Brandes AA, Marosi C, Bogdahn U, Curschmann J, Janzer RC, Ludwin SK, Gorlia T, Allgeier A, Lacombe D, Cairncross JG, Eisenhauer E, Mirimanoff RO (2005) Radiotherapy plus concomitant and adjuvant temozolomide for glioblastoma. N Engl J Med 352(10):987–996

Tacke J (2001) Thermal therapies in interventional mr imaging Cryotherapy. Neuroimaging Clin N Am 11(4):759–765

Thomson KR, Cheung W, Ellis SJ, Federman D, Kavnoudias H, Loader-Oliver D, Roberts S, Evans P, Ball C, Haydon A (2011) Investigation of the safety of irreversible electroporation in humans. J Vasc Interv Radiol 22(5):611–621

Young BD, Levine JM, Porter BF, Chen-Allen AV, Rossmeisl JH, Platt SR, Kent M, Fosgate GT, Schatzberg SJ (2011) Magnetic resonance imaging features of intracranial astrocytomas and oligodendrogliomas in dogs. Vet Radiol Ultrasound 52(2):132–141